

# Nonlinear Viscoelasticity of a Vulcanized Elastomer

E. KONTOU

Department of Theoretical and Applied Mechanics, The National Technical University of Athens, GR-15773, Athens, Greece

## SYNOPSIS

The material nonlinearities in the viscoelastic behavior of rubbers at modest-to-large deformations have been studied. A vulcanized network based on the styrene-butadiene elastomer has been tested in stress-relaxation experiments at room temperature for a wide range of deformations. After time-strain separability was confirmed, the damping function could be calculated and introduced into the Boltzmann superposition integral. The equilibrium stress-strain behavior of the system could then be described, while comparison with other theoretical equations has also been made. © 1994 John Wiley & Sons, Inc.

## INTRODUCTION

The viscoelastic behavior of rubbers at modest-to-large deformations is complicated by material nonlinearities. These nonlinearities arise either from stress vs. strain nonlinearities or from the dependence of the relaxation spectrum on the state of strain or both.<sup>1</sup> For the description of the nonlinear viscoelastic behavior of rubbers, two main constitutive theories applicable to engineering problems have been developed<sup>2</sup>: a modified version of the finite linear viscoelasticity (FLV) theory developed by Coleman and Noll<sup>3</sup> and the Chang, Bloch, and Tschoegl (CBT) theory,<sup>4-6</sup> which employs the generalized strain measure.

Chang et al. introduced a linear integral theory, which described successfully the viscoelastic behavior of cross-linked and uncross-linked styrene-butadiene rubbers (SBR) and uncross-linked polyisobutylene. In their theory, the relaxation spectrum is assumed to be independent of the state of strain, and the model can be applied to both large and small deformations.

According to their data,<sup>4</sup> the effects of time and strain are separable at moderate strains in both uniaxial and multiaxial stress-relaxation or creep curves. Moreover, by introducing a nonlinear measure of strain (parameter  $n$ ) into the Boltzmann superposition integral, they could accurately predict

the viscoelastic behavior of rubberlike materials, if the relaxation spectrum remains unchanged during the deformation.

The fundamental difference in the two theories is that the CBT theory is based on the assumption that the effects of strain and time are separable for all deformations including moderately large ones, whereas the modified FLV theory assumes separability only in the infinitesimal deformation regime. The FLV theory contains three steady-state functions of the three principal strain invariants and 12 relaxation functions of these invariants. For a certain class of incompressible materials exhibiting separability of time and strain effects under small deformations, the FLV theory can be simplified.

The CBT equation has the advantage of being simple in form, needing only two parameters to be evaluated before application. In simple uniaxial tension, the constitutive equation derived by Chang et al. reads

$$\sigma(t) = [2/(3n)] \int_0^t E^0(t - \tau)(d/d\tau) \times [\lambda(\tau)^n - \lambda(\tau)^{-n/2}] d\tau \quad (1)$$

where  $E^0(t)$  is the relaxation modulus, and  $n$ , the strain parameter.

Both theories yield good agreement with test data,<sup>2</sup> where material parameters derived from fitted uniaxial elastic data are used to predict the elastic response in pure shear.

The measure of strain with which the description of the mechanical properties of a given material can be cast in the simplest form is a characteristic of the material.

The equilibrium response of an elastomeric material represents only a part of the overall mechanical behavior. The stress observed upon deformation typically includes a significant contribution from dissipative processes.<sup>7</sup> The experimental characterization of these viscous effects requires fast displacement and observation of test specimens due to the rapid initial dissipation; viscous contributions can persist with diminished magnitude for long time periods. An infinite sum of exponentials is sometimes employed to fit relaxation data from polymeric materials, in consideration of the occurrence of a range of motions and corresponding relaxation processes. The longest time relaxation in cross-linked rubber networks is governed by the release of entanglement constraints on dangling network chains.<sup>8,9</sup>

Since reptation of the network strands is suppressed, a principal release mechanism is that of fluctuations in the contour length. The dangling chain retracts and reemerges from the tube of entanglements and thereby can assume a relaxed configuration. An empirical stress-relaxation function in which the stress has an inverse power law dependence on time has enjoyed wide success.<sup>9,10</sup>

In an analogous effort to generalize the Boltzmann superposition principle to provide at least a qualitative understanding of many nonlinear effects, various models of FLV have been proposed, in which the infinitesimal strain tensor is replaced by a finite measure of strain.<sup>11</sup> One such model is Lodge's,<sup>12</sup> in which the Finger tensor is used as the measure of deformation. This model can be written as follows:

$$\sigma_{ij}(t) = \int_0^t m(t-t')B_{ij}(t-t') dt' \quad (2)$$

where  $m(t-t')$  is the memory function, and  $B_{ij}$ , the component of the Finger tensor.

The memory function is related to the relaxation modulus of the Boltzmann superposition principle as follows:

$$m(t-t') = \frac{dE(t-t')}{dt'} \quad (3)$$

Thus, the memory function can, in principle, be obtained from any linear viscoelastic material function for the material of interest. For the generalized

Maxwell model representation of linear behavior, it is a sum of exponentials.

However, this model does not provide a quantitatively correct description for large departures from linearity. A scheme extensively used in the analysis of nonlinear data is the one developed by Wagner,<sup>13</sup> in which a damping function is used that is a function of the scalar invariants of the Finger tensor. This model is expressed by the equation

$$\sigma_{ij}(t) = \int_0^t m(t-t')h(I_1, I_2)B_{ij}(t, t') dt' \quad (4)$$

The damping function is obtained by fitting experimental data and is thus a nonlinear material function.

In simple shear experiments, it is possible to determine only a shear function  $h(\gamma)$ , whereas in simple extension, only an exponential damping function  $h(\epsilon)$  can be determined. Although it is possible to obtain a general form of the damping function, there is nothing unique about it. Therefore, it must be considered here to be simply a characterizing function for the empirical description of nonlinear behavior in experiments with given kinematics.

Wagner,<sup>14</sup> in order to describe nonlinear data, using the Lodge rubber-like liquid model, determined the form of the damping function that yields "neutral" (i.e., neither strain hardening nor strain softening) behavior as follows:

$$h(\epsilon) = \frac{3\epsilon}{e^{2\epsilon} - e^{-\epsilon}} \quad (5)$$

Wagner<sup>15</sup> also fitted the following damping function to Meissner's data<sup>16</sup>:

$$h(\epsilon) = [\alpha e^{2\epsilon} + (1-\alpha)e^{m\epsilon}]^{-1} \quad (6)$$

where  $\alpha$  and  $m$  are adjustable parameters.

In the present work, the nonlinear viscoelastic behavior of a cross-linked elastomeric network has been studied by means of stress-relaxation experiments covering a wide range of deformations. After the time-strain separability has been checked, the damping function  $h(\epsilon)$  could be obtained experimentally. Comparison with the corresponding theoretical expressions has been made and the best-fitted expression was introduced into the Boltzmann superposition integral for the most accurate prediction of the viscoelastic behavior of the elastomeric network tested.

## EXPERIMENTAL

A compound mixture of an elastomer SBR 1102 (supported by Shell Co.) has been used, with a system of two accelerators, namely, benzothiazyl disulfide (MBTS) and diphenyl guanidine (DPG). The ingredients recipe was as follows: SBR 1102: 100 phr; ZnO: 2 phr; stearic acid: 2 phr; MBTS: 0.4 phr; DPG: 0.2 phr; sulfur: 2 phr.

MBTS, as the primary accelerator, enhances the degree of cross-linking, while DPG activates MBTS. The ingredients were mixed in a Brabender mixer and the vulcanization was completed in a thermopress. The curing conditions were 150°C for 30 min. Dog-bone specimens about 2 mm thick were used in all types of experiments.

Stress-relaxation experiments were carried out at room temperature in a conventional Instron type 1121 tester as follows: The sample was prestressed up to a stretch ratio equal to 4 in order to avoid stress-softening effects and it was allowed to relax for a few days. Then, the sample was subjected to an initial elongation of 10 mm, which corresponds to a stretch ratio equal to 1.23, with a crosshead speed of 200 mm/min.

The Instron panel was modified to allow interfacing to a personal computer for full information of the test. The variation of load vs. time was recorded with a sampling rate of 1.8 pt/s over a period of 8 h. Data recorded within the first 10 s after the initial application of strain were not used in calculations to ensure that a true state of stress is being observed.<sup>17</sup> Successively, the second step of elongation was imposed after 24 h relaxation of the previous state, and the same procedure was followed up to a stretch ratio equal to 3.25. The stress variation with time for various values of the stretch ratio  $\lambda$  is presented in Figure 1.

In addition, nonequilibrium deformation experiments were executed at a constant crosshead speed velocity of 10 mm/min and were consistent with a uniaxial extension to a maximum stretch ratio equal to 3. The corresponding plot of this stress-strain test is displayed in Figure 5.

## RESULTS AND DISCUSSION

The stress-relaxation experiments as described above are presented in Figure 2, plotted as  $\log \sigma(t)$  vs.  $\log t$  for various values of the stretch ratio  $\lambda$ . Stress  $\sigma$  is the engineering stress (force/original cross-sectional area). From the almost parallel curves, it is clear that the time-shift invariance is

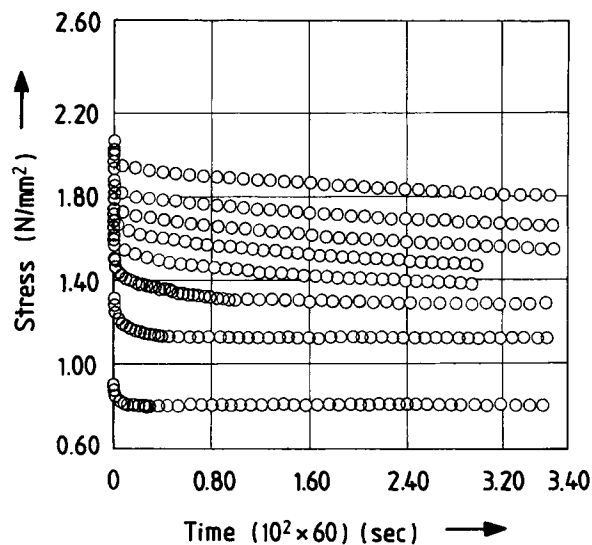


**Figure 1** Stress-relaxation experiments with varying the stretch ratio.

preserved for this type of deformation and this type of elastomeric network.

Therefore, the experimental damping function  $h(\epsilon)$  could be obtained from the vertical shifting of these plots.<sup>18</sup> Figure 3 shows the experimental damping function, which tends to unity for small deformations and is a decreasing function of the stretch ratio  $\lambda$ .

In comparison to the experimental data, the theoretical curves of  $h(\epsilon)$  according to eqs. (5) and (6) are also plotted. The best fit is observed with the use of eq. (6), where parameters  $a$  and  $m$  take the values 0.1 and 3, respectively.

By selecting a suitable fickle time (in our case,  $t = 20$  min), the stress  $\sigma$  as a function of the stretch ratio  $\lambda$  may be plotted, as shown in Figure 4, where each experimental point represents a separate experiment. In the same figure, the isochronal type of eq. (4) has also been plotted with the use of the damping function as expressed by eq. (6).

For the entire range of the imposed deformation, this equation fits the experimental data very well after a proper selection of the relaxation modulus  $E(t)$ . The predictions of the elastic behavior of an ideal rubber are also plotted as a dashed line in Figure 4 based on the equation

$$\sigma(t, \lambda) = E(t)(\lambda^2 - \lambda^{-1}) \quad (7)$$

Equation (7) fits the experimental data only at low values of the stretch ratio.

By using the isochronal form of eq. (1),

$$\sigma(\lambda) = (2/3n)E(t)[\lambda^{n-1} - \lambda^{-(n+2)/2}] \quad (8)$$

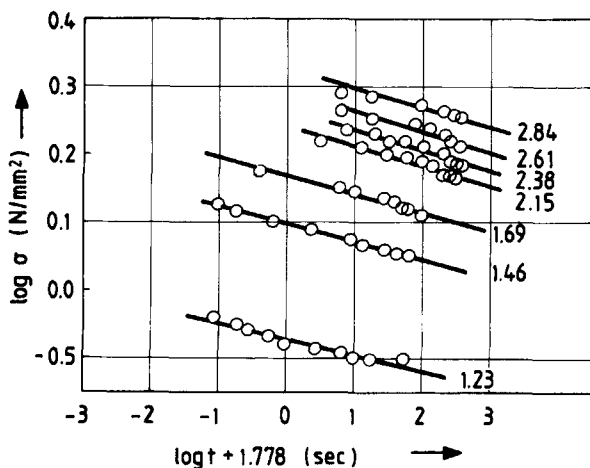


**Figure 2** Logarithmical plots of stress-relaxation data of Figure 1 in simple extension for various values of the stretch ratio  $\lambda$ .

the validity of this model was also tested with the data of Figure 4. The fit of eq. (8) to the experimental data of Figure 4 has been made with the strain parameter  $n$  taking the value 1.2. The selection of the relaxation modulus for the fit of the initial values of the curve could not lead to a description of the overall behavior of the system up to  $\lambda = 3$ .

The nonequilibrium stress-strain data, obtained as described above, are presented in Figure 5. By introducing the empirical formula of  $h(\epsilon)$ , given by eq. (6), in the integrals of eq. (4), a good approximation to the nonequilibrium experimental data is testified, as shown in Figure 5.

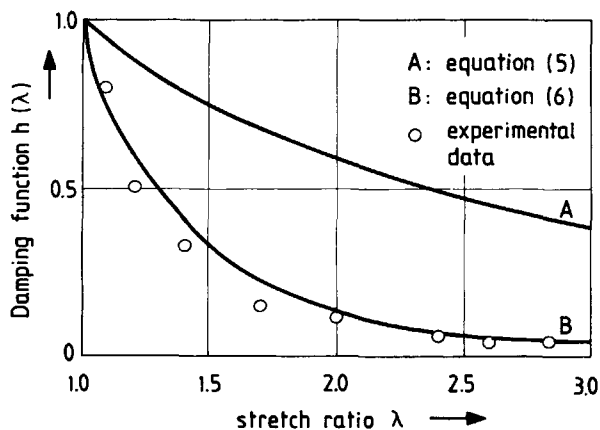


**Figure 3** The damping function  $h(\lambda)$  plotted against the stretch ratio  $\lambda$ .

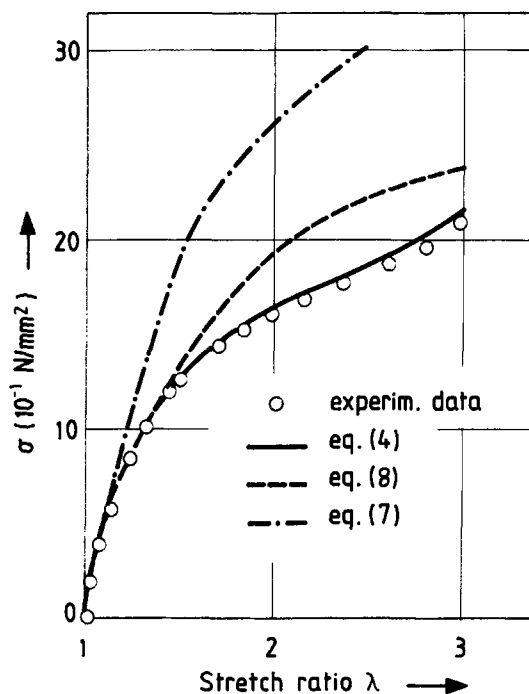


**Figure 4** Equilibrium stress-strain curve obtained from data of Figure 1 at  $t = 20$  min.

The relaxation modulus function adopted for the curve fitting of the experimental results has the well-known form

$$E(t) = E_0 \exp \left[ - \left( \frac{t}{\tau} \right)^b \right] \quad (9)$$

where  $\tau$  is the mean relaxation time and constant  $b$  expresses the distribution of relaxation times. This expression is equivalent to a series of Maxwell models proposed for the description of stress relaxation in the linear viscoelastic case. Constant  $b$  takes the value of 0.25, which is reasonable for this type of elastomer.

## CONCLUSIONS

From the above experimental results and comparison to the theoretical expressions, it is concluded that the effects of time and strain are separable at moderate strains in uniaxial stress-relaxation curves for the vulcanized SBR elastomer tested. Then, the stress can be factored out into a strain-dependent part  $h(\epsilon)$  and a time-dependent part  $E(t)$ .

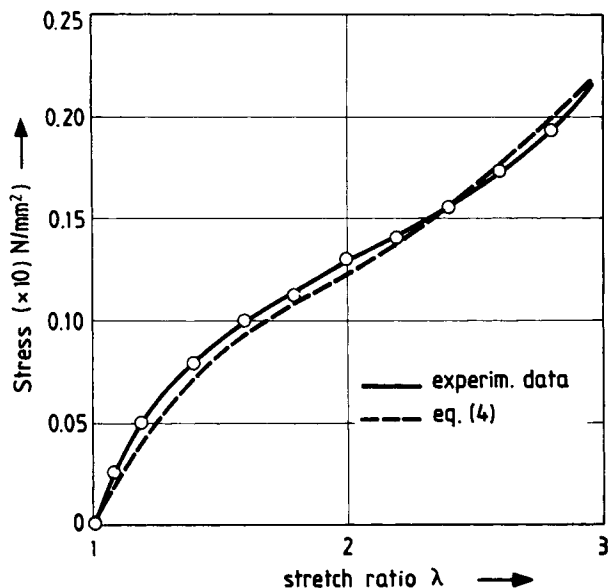


**Figure 5** Stress-strain curve of the elastomer tested in simple extension at a rate of deformation of 10 mm/min. Solid line: experimental data. Dashed line: prediction of eq. (4).

The experimental damping function  $h(\epsilon)$  was in agreement with Wagner's empirical formula. By introducing this function into the general form of stress, the viscoelastic behavior of the system could be described, resulting in an equilibrium stress-strain curve reasonably close to the experimental one.

## REFERENCES

1. J. L. Sullivan, *Soc. Rheol.*, **31** (3), 271 (1987).
2. J. L. Sullivan, K. N. Norman, and R. A. Pett, *Rubb. Chem. Technol.*, **53** (5), 805 (1980).
3. B. D. Coleman and W. Noll, *Rev. Mod. Phys.*, **33**, 239 (1961).
4. W. V. Chang, R. Block, and N. W. Tschoegl, *J. Polym. Sci. Phys. Ed.*, **15**, 923 (1977).
5. R. Block, W. V. Chang, and N. W. Tschoegl, *J. Rheol.*, **22** (1), 132 (1978).
6. W. V. Chang, R. Block, and N. W. Tschoegl, *Rheol. Acta*, **15**, 367 (1976).
7. C. M. Roland, *Rubb. Chem. Technol.*, **62** (5), 880 (1989).
8. J. D. Ferry, *Viscoelastic Properties of Polymers*, Wiley, New York, 1980.
9. M. Doi and S. F. Edwards, *The Theory of Polymer Dynamics*, Clarendon Press, Oxford, 1986.
10. T. G. Nutting, *J. Franklin Inst.*, **191**, 679 (1921).
11. J. M. Dealy, *Soc. Rheol.*, **34** (7), 1133 (1990).
12. A. S. Lodge, *Elastic Liquids*, Academic Press, London, 1964.
13. M. H. Wagner, *Rheol. Acta*, **15**, 136 (1976).
14. M. H. Wagner, *Rheol. Acta*, **18**, 33 (1979).
15. M. H. Wagner, *J. Non-Newton. Fluid. Mech.*, **4**, 39 (1978).
16. J. Meissner, *Rheol. Acta*, **10**, 230 (1978).
17. T. L. Smith, *J. Polym. Sci.*, **17**, 2181 (1979).
18. K. Osaki and M. Kurata, *Macromolecules*, **13**, 671 (1980).

Received February 15, 1994

Accepted May 30, 1994